Journal of Atmospheric and Solar-Terrestrial Physics xxx (2017) 1–8

Contents lists available at ScienceDirect

Journal of Atmospheric and Solar-Terrestrial Physics

journal homepage: www.elsevier.com/locate/jastp

# On a role of quadruple component of magnetic field in defining solar activity in grand cycles

E. Popova [a, b], V. Zharkova [c, *], S. Shepherd [d], S. Zharkov [e]

[a] Federal State Budget Educational Institution of Higher Education M.V.Lomonosov Moscow State University, Skobeltsyn Institute of Nuclear Physics, Russia
[b] Schmidt Institute of Physics of the Earth of the Russian Academy of Sciences, Russia
[c] Department of Mathematics, Physics and Electrical Engineering, Northumbria University, Newcastle upon Tyne, NE1 8ST, UK
[d] School of Engineering, Bradford University, Bradford, BD7 1DP, UK
[e] Department of Physics and Mathematics, Hull University, Kingston upon Hull, HU67RS, UK

ARTICLE INFO

*Keywords:*
Sunspots
Magnetic field
Solar activity cycle
Principal component analysis
Solar dynamo
Gleissberg cycle
Grand cycle

ABSTRACT

In this paper we revise our prediction of solar activity using a solar background magnetic field as a proxy by the inclusion of eigen vectors of solar magnetic waves produced by quadruple magnetic sources, in addition to the principal eigen modes generated by two-layer dipole sources (Zharkova et al., 2015). By considering the interference of two dipole and one quadruple waves we produce the revised summary curve for the last 400 years accounting for the additional minima of solar activity occurred at the beginning of 19th (Dalton minimum) and 20th centuries. Using the dynamo model with meridional circulation and selecting the directions of circulation for quadruple waves, we estimate the parameters of quadrupole waves best fitting the observations in the past grand cycle. The comparison shows that the quadruple wave has to be generated in the inner layer of the solar convective zone, in order to provide the additional minima observed in 19 and 20 centuries, thus, naturally accounting for Gleissberg centennial cycle. The summary dynamo wave simulated for the dipole and quadruple sources reveals much closer correspondence of the resulting summary curve derived from the principal components of magnetic field variations to the solar activity oscillations derived from the average sunspot numbers in the current grand cycle.

## 1. Introduction

Solar magnetic activity is manifested with the appearance of sunspots on the solar surface of the Sun with relatively complicated structure having the main period of about 22 years. The monthly sunspot numbers averaged from observations by many observatories show quasi-regular maxima and minima of solar activity appearing with changing leading magnetic polarity in each hemisphere approximately every 11 years or with the same polarity about every 22 years (Hathaway et al., 2002). The longest direct observation of solar activity is the 400-year sunspot-number series, which depicts a dramatic contrast between the almost spotless Maunder and Dalton minima, and the period of very high activity in the most recent 5 cycles (Solanki et al., 2004; Solanki and Krivova, 2011).

Observations of many cycles consistently show essential differences between activity in the opposite hemispheres for sunspots (Zharkov et al., 2008), active regions (Jennings and Weiss, 1991; Jennings, 1991), solar flares (Zharkov and Zharkova, 2011), solar and heliospheric magnetic fields Bravo and González-Esparza (2000) and geomagnetic activity (Murayama and Nosaka, 1991). However, the accurate sunspot observations recorded at the Observatoire de Paris during Maunder minimum from 1660 to 1719 (Ribes and Nesme-Ribes, 1993) demonstrated that the solar magnetic field was completely strongly asymmetric with respect to the solar equator with sunspots occurring only in one hemisphere and within a narrow latitude band hardly exceeding 20 degrees of latitude.

Prediction of a solar cycle through sunspot numbers has been used for decades as a way of testing knowledge of mechanisms of solar dynamo, including the processes providing production, transport and disintegration of the solar magnetic field. The records show that solar activity in the current cycle 24 is much lower than in the previous three cycles 21–23 revealing more than a two-year minimum period between cycles 23 and 24.

However, most predictions of solar activity by various methods considering linear regression analysis (Pesnell, 2008), neural network forecast (Maris and Oncica, 2006), modified flux-transport dynamo model calibrated with historical sunspot data from the middle-to-equator

* Corresponding author.
*E-mail address:* valentina.zharkova@northumbria.ac.uk (V. Zharkova).

http://dx.doi.org/10.1016/j.jastp.2017.05.006
Received 3 January 2017; Received in revised form 7 April 2017; Accepted 6 May 2017
Available online xxxx
1364-6826/

latitudes (Dikpati et al., 2006), anticipated a much stronger cycle 24 (Pesnell, 2008). There were only a few predictions of the weaker cycle 24 (Choudhuri et al., 2007) obtained with the high diffusivity Babcock-Leighton dynamo model applied to polar magnetic fields as a new proxy of solar activity.

This systematic deviation of the predicted sunspot activity from the one actually measured in cycle 24 indicates some significant discrepancy between the processes used in the prediction compared to the real ones defining a solar activity cycle through the action of solar dynamo. It was also discovered Karak and Nandy (2012) that a dynamo model cannot produce reliable prediction of solar activity for longer than one solar cycle because of a 'short memory' of 'mean' dynamo.

More definitive information about solar background magnetic fields was recently obtained with the Principal Component Analysis (PCA) (Zharkova et al., 2012) applied to low resolution whole disk magnetic data for cycles 21–23 observed with the Wilcox Solar Observatory (WSO) using their variance as the main classifier. This allowed the authors to obtain more than 8 significant eigen vectors of solar magnetic field oscillations, which came in pairs. The pair with the highest eigen values, or highest variance, was used to define the two principal components of the opposite polarities traveling from one hemisphere to another with close but not equal frequencies (Zharkova et al., 2012; Shepherd et al., 2014) generated in two cells of the solar interior (Zhao et al., 2013).

These PCs are assumed to be magnetic waves produced by a dipole magnetic source of the Sun (Zharkova et al., 2012; Popova et al., 2013). In addition, there were three other pairs of secondary magnetic field components with slightly smaller than dipole amplitudes related to quadruple magnetic sources which have a decreasing amplitude and increasing phase difference with an increasing cycle number (Zharkova et al., 2012).

By applying the symbolic regression analysis for periodic functions to these two PCs (Schmidt and Lipson, 2009), their parameters and summary curve were derived (Shepherd et al., 2014) and shown to be a good alternative proxy of solar activity, instead of sunspots. This summary curve was expanded to 800 years backwards fand 1200 years forward to reveal a grand cycle of solar activity of 350–400 years caused by a beating effect of these PCs with the grand minima coinciding with Maunder and Wolf and other minima of solar activity in the past millennium. The next grand minimum is shown to approach in cycles 25–27 (Zharkova et al., 2015). This analysis helped the authors to understand the important role of solar dynamo waves originating from the two different layers in the solar interior: at the bottom of the convection zone and in the shallow region below the solar surface.

However, this summary curve did not predict accurately the occurrence of Dalton minimum and another similar minimum occurred at the beginning of 20 century as well as Sporer minimum in the current grand cycle (1655–2020) as indicated in the comments by Usoskin and Kovaltsov (2015) placed below our original paper (Zharkova et al., 2015). To explain this missing Sporer minimum the extended paper is submitted (Zharkova et al., 2017) describing the discrepancies between our summary curve and the activity curve derived with carbon dating (Usoskin et al., 2004) in Sporer minimum by specific extra-terrestrial conditions (supernova radiation), affecting the terrestrial biomass, from which carbon dating is derived. However, in the current paper we attempt to resolve another issue, namely, not clear Dalton minimum in the summary curve, which, we believe, is related to the effect of missing quadruple magnetic waves in the previous interpretation (Zharkova et al., 2015).

The magnetic waves generated by quadruple magnetic sources not considered by Zharkova et al. (2015) can affect the appearance of sunspots by interacting with dipole waves and causing another beating, or double beating effect reported by Zharkova et al. (2015). This double beating effect can change the appearance of a grand cycle presented in paper (Zharkova et al., 2015) and produce some additional minima not accounted for in the dipole model. In order to include quadruple waves we need to utilize the relevant dynamo modelling because the observational quaruple waves are not yet classified by the symbolic regression analysis.

For this reason we use the suggestion that magnetic activity is associated with the action of a solar dynamo as proposed by Parker (1955) combining the effects of magnetic field shear and stretching caused by the differential rotation ($\omega$-effect) and twisting of magnetic flux loops over the solar interior depths allowing them to appear on the surface at particular latitudes ($\alpha$-effect). Such representation provides the solution of dynamo equations in a form of oscillating waves of: a) the poloidal (background) magnetic field traveling from pole to pole in the whole Sun and b) the toroidal (sunspot) magnetic fields (dynamo-waves) appearing from the middle latitudes to the equator.

A toroidal magnetic field is produced from the poloidal field by the action of differential rotation. The inverse process of transforming toroidal magnetic field into poloidal field occurs due to the breaking mirror symmetry by the convection in the rotating Sun. The action of the Coriolis force on expanding, rising (compressed and sinking) vortices results in a predominance of right-handed vortices in the Northern hemisphere and left-handed vortices in the Southern hemisphere. After averaging over velocity pulsations, the electromotive force produced by Faraday electromagnetic induction acquires a component $\alpha\mathbf{B}$ parallel to the mean magnetic field $\mathbf{B}$. This mechanism for generating magnetic fields is the one called '$\alpha-\omega$ dynamo'.

Parker (1955) assumed that generation of a dynamo process occurs in a single spherical shell, where twisting of the magnetic field lines ($\alpha$-effect) and magnetic field line stretching and wrapping around different parts of the Sun owing to its differential rotation ($\omega$-effect) are acting together. However, the locations of the $\alpha$-effect are likely to be displaced from that of the shear. Moreover, as shown by the helioseismological observations, in some regions of the convective zone the latitudinal shear dominates over the radial shear and there are at least two shells in the solar interior (Zhao et al., 2013) where the dynamo waves can be produced (Zharkova et al., 2015).

In addition, a meridional circulation is expected to include at least two opposing contributions: one is a flow, which transports solar plasma, say, from the equator to the pole near the surface, and the other is a deeper counter-flow, which returns the plasma to the equatorial region that makes the mass distribution stationary. This process associates the dynamo generators with different radial layers and consequently, the radial variable needs to be included into the dynamo-governing equations for two radial layers where dynamo waves are generated (Parker, 1993; Popova et al., 2013).

Another approach is used by Babcock (1961) suggesting the model with the meridional circulation, which governs the origin of dynamo waves. The model for active region appearances and decays was mathematically defined and analyzed by Leighton (1969). This model was subsequently developed by Wang et al. (1991), followed by Durney (1995); Choudhuri et al. (1995), who built flux transport models with the meridional flows in the convective zone.

Given the complexity of the physics in the interior of the Sun, in order to comply with observations, any model should be able to simulate the important features of typical solar cycle (Choudhuri et al., 2004; Dikpati et al., 2004), such as the butterfly diagram, and the phase relation in time between toroidal (sunspot) fields and poloidal (polar) fields. The dynamo models are expected to be calibrated with solar observations by complying with the differential rotation and the meridional circulation that are close to that observed in the Sun.

Recently, a dynamo-based predictive tool was built (Dikpati et al., 2006) by converting Babcock-Leighton's calibrated flux-transport dynamo model into a linear system forced from the surface (and not from the convective zone) and applied it to predict the relative sequence of peaks of solar cycles 12 through 24. By assimilating into the model the surface magnetic-flux data since cycle 12 up to cycle 23, Dikpati et al. (2006) have shown that the first four cycles are required to build its magnetic memory enabling correct prediction of the relative sequence of peaks of cycles 16 through 23. Although, this model failed to predict

correctly the current very weak solar cycle 24.

Also there is a different class of flux transport dynamos, where the flux transport is shared, at least, equally by circulation and turbulent diffusion (Choudhuri et al., 2007; Karak and Nandy, 2012; Muñoz-Jaramillo et al., 2013). In fact, the two classes of models yielding very different predictions of the solar cycle, still are unable to predict the magnetic activity for longer than a single solar cycle of 11 years (Karak and Nandy, 2012; Muñoz-Jaramillo et al., 2013). The similar trend occurs in many other models using various spectral analysis and artificial intelligence methods applied for prediction of solar activity based on the sunspot observations (see, for example Pesnell, 2008, and references therein). This indicates that the simplified definition of solar activity with averaged sunspot numbers is not fully functional that requires to develop a new approach.

Helioseismic measurements of the Sun's inner rotation near the poles at the bottom of turbulent dynamo at the maximum phase of cycle 23 have shown the physical conditions in deep layers of the solar convection zone to be favourable for exciting a quadrupole mode of poloidal magnetic field (Kryvodubskyj, 2001). Also Sokoloff and Nesme-Ribes (1994) have shown that an azimuthal field can be generated in a non linear regime from a dominant dipole and a weak quadrupole mode leading to a small north-south asymmetries in the field strength often observed in the solar activity. Furthermore, the existence of joint solution for dipole and quadrupole components with the similar amplitudes can lead to the absence of sunspot activity in the other hemisphere (Sokoloff and Nesme-Ribes, 1994) that was observed during Maunder minimum (Ribes and Nesme-Ribes, 1993). Hence, quadruple magnetic sources can be essential in defining the observational features of solar activity.

In the current paper we intend to utilize the principal components derived from the WSO magnetic field observations (Zharkova et al., 2012) and simulated dynamo waves associated with dipolar magnetic sources generated in the two cells of the solar interior (Zhao et al., 2013) and to add to them a quadruple component derived from the double dynamo model used in modelling of poloidal and toroidal magnetic fields for a solar dipole (Zharkova et al., 2015). The summary of observations is presented in section 2, the governing equations for simulation of dynamo waves of the poloidal magnetic field considering joint dipole and quadruple magnetic sources are discussed in section 3, the estimation of beating periods and location of the wave sources are presented in section 4 and conclusions are drawn in section 5.

## 2. Principal components derived from the observed magnetic field variations

In our previous paper (Zharkova et al., 2015) the original magnetic field data from full disk magnetograms for the 3 solar cycles (21–23) was checked using principal component analysis (PCA) classified by the data variance. This allowed us to derive a significant ($> 8$) number of the eigen values and eigen vectors describing various types of waves present in solar magnetic field oscillations. The most surprising outcome of this exercise was that these eigen values and vectors came in pairs. The pair with the highest variance two assigned to the two principal components (PCs) associated with the waves produced by dipole magnetic sources acting in two different layers of the solar interior (inner and outer ones). These waves were considered to be double dynamo waves produced by the dipole magnetic sources of the Sun. This assumption was confirmed by the simulation of two dynamo waves from these two layers different directions of meridional circulation reproducing rather closely the observational PCs(Zharkova et al., 2015). One the layers is assumed to be at the bottom of the solar convective zone (SCZ) and another one close to the solar surface, similar to the two cells reported from helioseismic observations (Zhao et al., 2013).

Our findings revealed the very stable magnitudes of eigen values of these two dynamo waves for the solar cycles (21–23) considered, whether they derived from a single cycle, or from a pair of cycles in any combination, or from all three of them (21–23) (Zharkova et al., 2015). This proves that the parameters of the own oscillations of the Sun in these two layers, as well as the parameters of their summary curve presented in Fig. 3 of Zharkova et al. (2015) are closely maintained over a large period of time. This dismounts the suggestion of stochastic Sun put forward by Usoskin et al. (2004) and implemented into the restored solar activity curve presented in Solanki et al. (2004). Zharkova et al. (2015) calculate the summary curve of the two PCs (magnetic waves) (see their Fig. 3) for the period 1200− 3200 using the analytical formulae (2 and 3) from the Method of data analysis (Zharkova et al., 2015). The modulus summary curve, where negative magnetic fields were reflected into the positive ones, is shown to closely correlate with the average sunspot numbers in cycles 21–24 defining solar activity in its classic view (Shepherd et al., 2014; Zharkova et al., 2015).

The parameters of the waves generated in the two interior cells are found to have close but not equal frequencies, which vary periodically on a large timescale owing to different physical conditions in these two layers (Zharkova et al., 2015). These close frequencies are shown to cause the beating effect of these two waves of solar activity, which produces five of grand cycles in the two millennia (1200–3200) considered with the grand minima occurring every 350–400 years (Zharkova et al., 2015). These waves are also reproduced by the dynamo model using dipole magnetic sources in each layer (Zharkova et al., 2015), matching reasonably well the major minima of solar activity in the last millennium (Maunder, Wolf). It was also predicted (Zharkova et al., 2015) that the next grand minimum similar to Maunder one is approaching in the next cycles 25–27.

However, the summary curve by Zharkova et al. (2015) did not account for a few smaller minima of activity, e.g. Dalton minimum or the minimum at the beginning of 20th century. To demonstrate these discrepancies, in Fig. 1 (top plot) an extract is plotted for the current grand cycle (1655–2030) from the summary curve in Fig. 3 (Zharkova et al., 2015). A modulus summary curve representing the absolute value of magnetic field in the summary curve is plotted in Fig. 1 (middle plot) with Wolf's numbers derived from the observed averaged sunspot numbers plotted in Fig. 1 (bottom plot). The two vertical lines in Fig. 1 indicate the minima of solar activity at the beginning of 19th century (Dalton minimum) and at the early 20th century. It can be seen that the modulus summary curve (middle plot) does not reproduce these two minima.

In the next section we explain that these minima can be recovered by considering a quadruple component of magnetic waves produced in one of the two cells in the solar interior (Zhao et al., 2013). This suggestion is supported by helioseismic measurements of the physical conditions in deeper layers of the solar convection zone, which are shown favourable for exciting a quadrupole mode of poloidal magnetic field (Kryvodubskyj, 2001).

## 3. Governing equations for joint dipole and quadruple dynamo waves

In order to explain better the effects of background magnetic field on solar activity and to account for the two missing minima in the current grand cycle, we include into consideration the next set of independent components of solar magnetic field (Zharkova et al., 2012), which are produced by quadruple magnetic sources, in addition to the two principal components produced by a dipole magnetic source (Zharkova et al., 2015). However, the observational quadruple components are not yet distilled in analytical functions (Schmidt and Lipson, 2009) from the set of principal components derived by Zharkova et al. (2012) as it was done for the dipole components (Shepherd et al., 2014; Zharkova et al., 2015). Hence, the only way to include the quadruple components into prediction of solar activity is to reproduce them with the two-layer dynamo model similar to that reported in Zharkova et al. (2015).

For the dynamo wave simulations let us use the low mode approach. The basic idea of this approach follows the findings of principal component analysis (Zharkova et al., 2012, 2015), which reduced a

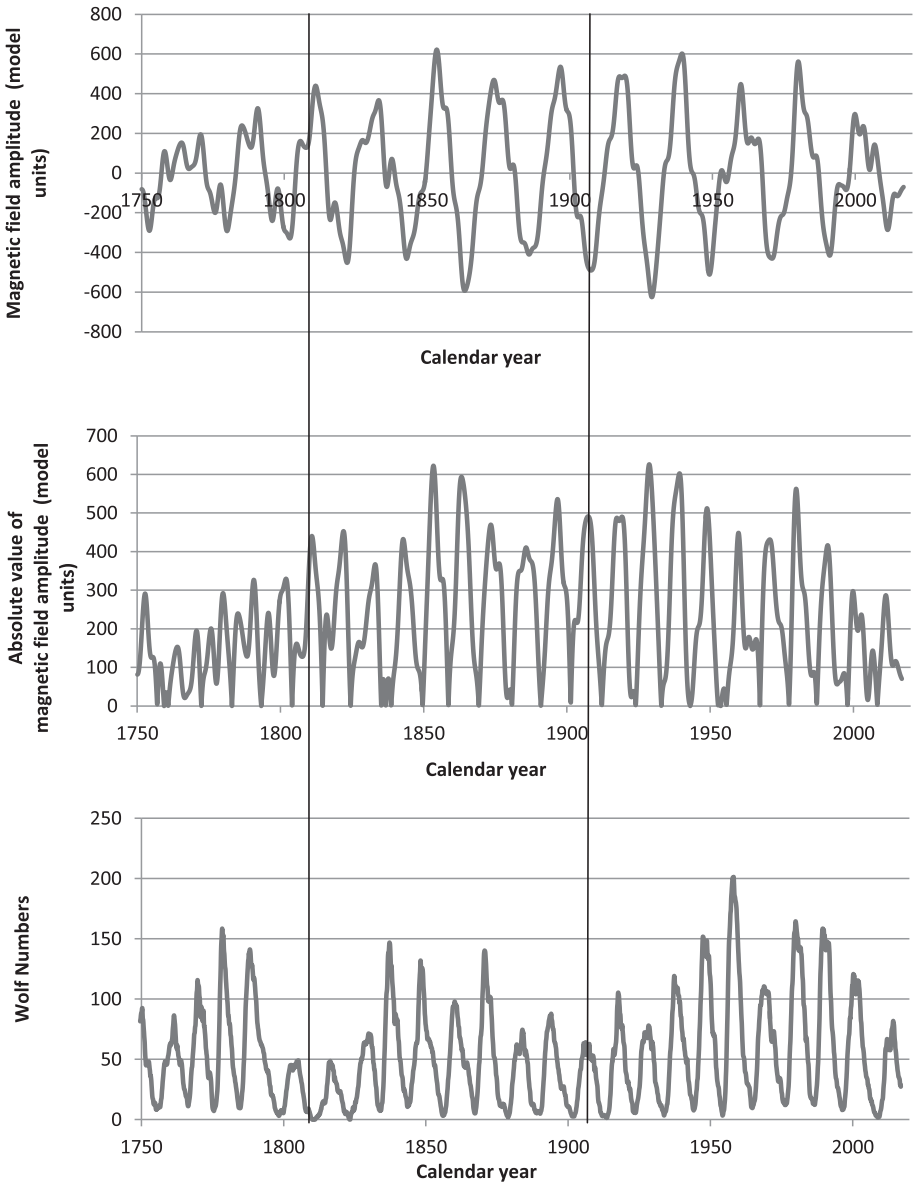


**Fig. 1.** Top plot: temporal variations of the resulting magnetic field amplitude for dipole magnetic source (the summary curve extracted from Fig. 3 (Zharkova et al., 2015)) for 1750–2016 years. Middle plot: temporal variations of the modulus summary curve obtained from the summary curve (in top plot) for magnetic field in 1750–2016 years. Bottom plot: the temporal variations of Wolf numbers derived from the observed averaged sunspot numbers.

dimensionality of solar magnetic waves by deriving their eigen values and corresponding eigen vectors from the full disc magnetic synoptic maps using the variance as a classifying factor. The similar approach can be applied in the dynamo modelling, where the mean-field dynamo equations are to be projected onto a minimum set of the eigenfunctions describing the variations of magnetic fields only related to these eigen vectors. In this case it is necessary to choose a minimum set of functions in such the way that the solution, which is a set of several time-dependent Fourier coefficients taking into account the generation sources, describes the general behavior of the magnetic field for this set of functions only (related to given eigen values) while omitting any functions with lower eigen values. By substituting the chosen set of magnetic field components into the dynamo equations one can obtain a dynamical system of equations containing the selected modes.

Following the previously described approach (Popova et al., 2013; Zharkova et al., 2015), let us consider the case when the dynamo waves of magnetic field are generated independently in two different layers in the solar interior, which are proven to exist following the findings from PCA by Zharkova et al. (2012, 2015) and from the helioseismological observations with the Solar Dynamic Observatory (SDO) payload by Zhao et al. (2013). In this case the dynamo equations describing dynamo waves in these two layers with meridional circulation can be written as follows:

$$\frac{\partial A_i}{\partial t} + V_i \frac{\partial A_i}{\partial \theta} = R_{\alpha i} B_i + \Delta A_i, \tag{1}$$

$$\frac{\partial B_i}{\partial t} + \frac{\partial (V_i B_i)}{\partial \theta} = R_{\omega i} \sin\theta \frac{\partial A_i}{\partial \theta} + \Delta B_i, \tag{2}$$

Here, $i$ is a number of the layer, $B$ is the toroidal magnetic field, $A$ is the vector potential of the poloidal magnetic field, proportional to the toroidal component and $\theta$ is the latitude measured from the pole. The factor $\sin\theta$ describes the decrease in the length of a line of latitude near the pole. The second equation neglects the small contribution of the $\alpha$-effect, i.e. we use so-called $\alpha\omega$ approximation. Curvature effects are absent in the diffusion terms. It is assumed that the radial gradient of the angular velocity does not vary with $\theta$.

In Eqs. (1) and (2) the parameters $R_\alpha$ and $R_\omega$ describe intensity of the $\alpha$-effect and the differential rotation, respectively. We used a simple scheme for the stabilization of the magnetic field growth, namely, the algebraic quenching of the helicity. This scheme assumes that $\alpha = \alpha_0(\theta)/(1+\xi^2B^2) \approx \alpha_0(\theta)(1-\xi^2B^2)$, where $\alpha_0(\theta) = \cos\theta$ is the helicity in the unmagnetized medium and $B_0 = \xi^{-1}$ is the magnetic field for which the $\alpha$-effect is considerably suppressed.

Let us consider the latitude distribution of the magnetic field for dipole magnetic sources in the form (Zharkova et al., 2015):

$$B(\theta,t) = b_1(t)\sin2\theta + b_2(t)\sin4\theta,$$
$$A(\theta,t) = a_1(t)\sin\theta + a_2(t)\sin3\theta$$

with the dipole symmetry conditions $A(0) = B(0) = A(\pi) = B(\pi) = 0$ .

By substituting the chosen set of components of magnetic field into the dynamo equations and collecting the coefficients of the sines with similar arguments, one can obtain a dynamical system of six equations containing the two dipole and one quadruple modes:

$$\dot{a}_1 = -a_1 + \frac{3}{2}va_2 - \frac{1}{2}va_1 - \frac{3}{8}R_\alpha\xi^2b_1^3 - \frac{3}{4}R_\alpha\xi^2b_1b_2^2 + \frac{1}{2}R_\alpha b_1, \quad (3)$$

$$\dot{a}_2 = \frac{1}{2}R_\alpha b_2 - \frac{1}{2}va_1 + \frac{1}{2}R_\alpha b_1 - 9a_2 - \frac{3}{4}R_\alpha\xi^2b_1b_2^2 - \frac{3}{4}R_\alpha\xi^2b_1^2b_2 - \frac{3}{8}R_\alpha\xi^2b_1^3 - \frac{3}{8}R_\alpha\xi^2b_2^3, \quad (4)$$

$$\dot{b}_1 = -4b_1 + \frac{1}{2}R_\omega a_1 - \frac{3}{2}R_\omega a_2 + vb_2, \quad \dot{b}_2 = -16b_2 + \frac{3}{2}R_\omega a_2 - 2vb_1, \quad (5)$$

Here, we use Newton's notation to define the time derivatives by applying dots above $a$ and $b$.

Then, in the case of the dipole and quadrupole symmetries the minimal set of the first eigenfunctions for reproducing solar cycle contains the six modes (Popova, 2013):

$$B(\theta,t) = b_3(t)\cos2\theta + b_4(t)\cos4\theta + b_5(t)\cos6\theta,$$
$$A(\theta,t) = a_3(t)\cos\theta + a_4(t)\cos3\theta + a_5(t)\cos5\theta$$

A dynamical system can be obtained in the similar way as for dipole sources shown above in eqs. (3)–(5), but expanding the terms to include the quadruple source contributions:

$$\dot{a}_1 = -\frac{3}{8}R_\alpha\xi^2b_2^2b_3 - \frac{3}{8}R_\alpha\xi^2b_1^2b_3 - \frac{3}{8}R_\alpha\xi^2b_1^3 - \frac{3}{4}R_\alpha\xi^2b_1b_3^2 - \frac{3}{4}R_\alpha\xi^2b_1^2b_2 + \frac{3}{2}va_2 + \frac{1}{2}R_\alpha b_1 - \frac{3}{4}R_\alpha\xi^2b_1b_2^2 - \frac{3}{2}R_\alpha\xi^2b_1b_2b_3 + \frac{1}{2}va_1 - a_1, \quad (6)$$

$$\dot{a}_2 = -\frac{3}{4}R_\alpha\xi^2b_2b_3^2 - \frac{1}{2}va_1 - \frac{3}{4}R_\alpha\xi^2b_1b_3^2 - \frac{3}{4}R_\alpha\xi^2b_1b_2^2 + \frac{1}{2}R_\alpha b_1 - \frac{3}{8}R_\alpha\xi^2b_1^3 - \frac{3}{8}R_\alpha\xi^2b_2^2b_3 + \frac{5}{2}va_3 - \frac{3}{4}R_\alpha\xi^2b_1b_2b_3 + \frac{1}{2}R_\alpha b_2 - \frac{3}{4}R_\alpha\xi^2b_1^2b_2 - \frac{3}{8}R_\alpha\xi^2b_2^3 - \frac{3}{8}R_\alpha\xi^2b_1^2b_3 - 9a_2, \quad (7)$$

$$\dot{a}_3 = -\frac{3}{4}R_\alpha\xi^2b_1b_2b_3 + \frac{1}{2}R_\alpha b_2 - \frac{3}{4}R_\alpha\xi^2b_2b_3^2 + \frac{1}{2}R_\alpha b_3 - \frac{3}{4}R_\alpha\xi^2b_2^2b_3 - \frac{3}{8}R_\alpha\xi^2b_1b_2^2 - \frac{1}{8}R_\alpha\xi^2b_1^3 - \frac{3}{8}R_\alpha\xi^2b_3^3 - \frac{3}{4}R_\alpha\xi^2b_1^2b_3 - 25a_3 - \frac{3}{2}va_2 - \frac{3}{8}R_\alpha\xi^2b_2^3 - \frac{3}{4}R_\alpha\xi^2b_1^2b_2, \quad (8)$$

$$\dot{b}_1 = -4b_1 + \frac{1}{2}R_\omega a_1 + vb_2 - \frac{3}{2}R_\omega a_2, \quad (9)$$

$$\dot{b}_2 = -2vb_1 + 2vb_3 - 16b_2 - \frac{5}{2}R_\omega a_3 + \frac{3}{2}R_\omega a_2; \quad (10)$$

$$\dot{b}_3 = \frac{5}{2}R_\omega a_3 - 36b_3 - 3vb_2; \quad (11)$$

## 4. Simulation results and Gleissberg cycle

### 4.1. Interference of dipole and quadruple waves and Gleissberg cycle

Using the dynamo model with meridional circulation described in 3 one can estimate the periods and approximate location of the wave sources in the depth of the SCZ. The periods of the waves derived from the dynamo model above are regulated by the amplitude of a meridional flow.

Let us estimate the periods of the resulting dynamo waves including the interference of two dipole and one quadruple waves to match the observed waves derived from sunspot observation (22 year cycle) (Hathaway et al., 2002), PCA (400 years grand cycle) (Zharkova et al., 2015) and Gleissberg cycle of about 100 years often reported in solar activity. We anticipate that these three cycles can be accounted for by the interference of these three waves. This interference is expected to cause the beating effect similar to the one described by Zharkova et al. (2015) when interpreting the summary curve from two layers in the solar interior produced dipole magnetic sources. This, in turn, can explain the occurrence of Dalton and other centennial minima caused by quadruple waves as Gleissberg cycle in solar activity.

Let us describe a simple calculation of the expected resulting periods, following the technique presented by Zharkova et al. (2015) (their formula (1) in section on beating effects). Any two interfering waves with the close cyclic frequencies $\omega_1$ and $\omega_2$ can produce a beating effect with their upper frequency, $\omega_u$ being the average of these two, $\omega_u = 1/2(\omega_1+\omega_2)$ and the lower frequency, $\omega_l$, being their difference, $\omega_l = 1/2(\omega_1-\omega_2)$. In result, the resulting wave has high frequency oscillations with the average frequency $\omega_u$ and low-frequency oscillations of its amplitude with the averaged frequency $\omega_l$, that constitutes the beating effect and occurrence of global minima with the period $T_l$, in addition to the regular oscillations with the period $T_u$.

By substituting the relation for cyclic frequency $\omega = 2\pi f = \frac{2\pi}{T}$, where $f$ is a normal frequency and $T$ is a period of wave, one can derive the formulae for the periods caused by the interaction of two waves, or the beating effects, $T_u = 2\frac{T_1T_2}{T_{2+}}T_1$ and $T_l = 2\frac{T_1T_2}{T_{2-}}T_1$. Here $T_1$ and $T_2$ are the original periods of the two interacting waves.

For the beating effect of three waves: two dipole waves with periods $T_1$ and $T_2$ and one quadruple wave with period $T_3$, one can derive the following expressions for the resulting periods of interfering waves:

$$T_{22} = 2\frac{T_1T_2}{T_2+T_1}; T_{GM} = \frac{T_1T_2}{T_2-T_1}; T_{sec} = \frac{T_1T_3}{T_3-T_1}, \quad (12)$$

where $T_{22}$ is the period of the 22-year cycle, period $T_{sec}$ corresponds to the Gleissberg cycle, and $T_{GM}$ corresponds to period of a grand cycle.

In order to match the observations and to achieve known periods of solar activity, e.g. $T_{22}\approx22$ years, $T_{sec}\approx100$ years, $T_{GM}\approx400$ years, one would need to have two dipolar waves with $T_1 = 21.41$, $T_2 = 22.62$, and one quadrupolar wave with $T_3 = 27.24$.

We carry out a detailed analysis of the magnetic field variations for 1700–2020 years (current grand cycle) because the observational data of solar activity in this period are fairly reliable. The resulting temporal variations of the modulus summary curve for dipole and quadrupole magnetic fields simulated with such the periods is shown in Fig. 2 (top

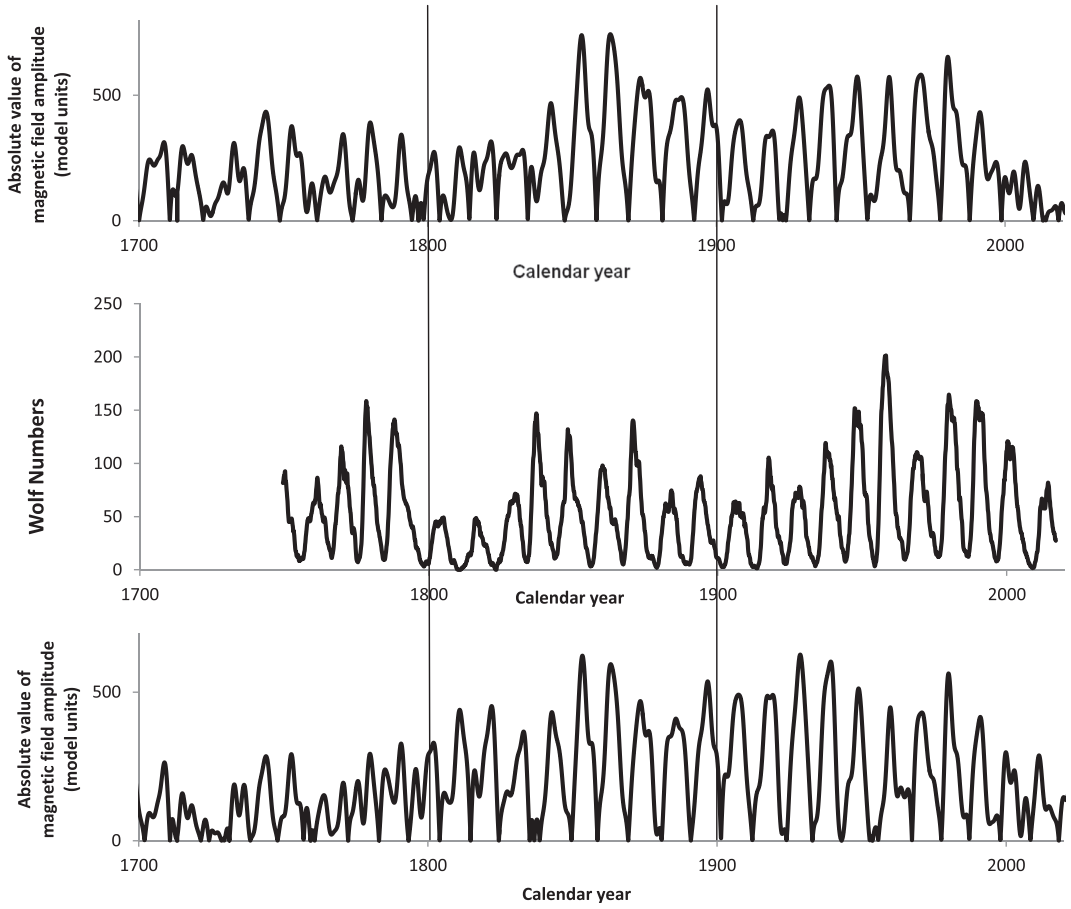


**Fig. 2.** Top plot: Temporal variations of the absolute value of summary curve derived for dipolar and quadrupolar magnetic field (updated modulus summary curve). Middle plot: Wolf numbers temporal variations for 1750–2016 years. Bottom plot: temporal variations of the original modulus summary curve of the resulting magnetic field (extracted from Fig. 3, (Zharkova et al., 2015)).

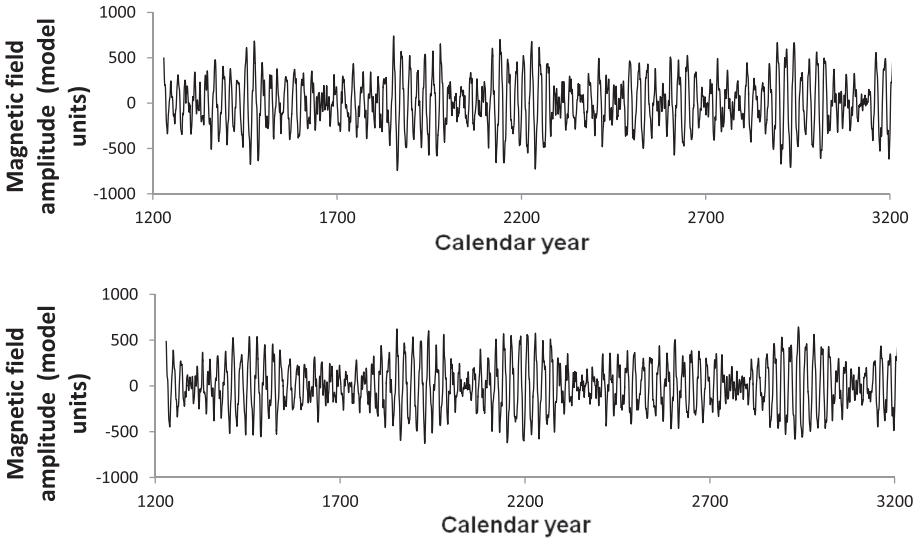


**Fig. 3.** Variations on a millennium timescale of the joint summary curve derived in the two layers: the original one derived for dipolar magnetic fields only (Zharkova et al., 2015) (bottom plot) and the updated one derived for the joint effect of dipolar and quadrupolar magnetic fields as described in the current study (top plot).

plot), the variations of Wolf numbers are shown in (middle plot), and variations of the summary curve for dipole sources extracted from (Zharkova et al., 2015) (their Fig. 3) for 1700–2020 years are plotted in Fig. 2 (bottom plot).

It can be seen that the simulations of the joint dipole and quadruple magnetic waves shown in Fig. 2(top plot) reproduce rather closely, as shown by the vertical lines, the two secular minima in the current grand cycle occurred at the beginning 19 (Dalton minimum) and 20 centuries. These seculiar minima occur with a period of about 100 years and defined as Gleissberg cycle, that is similar to those reported by the

observations (middle plot).

In order to reproduce the centennial minima of Gleissberg cycles to match the ones seen in Wolf number observations as shown in Fig. 2 (middle plot), and to make these seculiar minima slightly higher than the grand minimum (Maunder minimum), the quadrupole field amplitude is required to be a factor of 0.3 of the amplitude of the dipole field, following the conclusions by Sokoloff and Nesme-Ribes (1994). Our simulations show the period of Gleisberg cycle to range from 95 to 100 years that is governed by small variations of the period of a quadrupole wave between 27.24 and 28 years and its interference with the summary curve caused by the dipole sources in two layers.

Let us now extend these model simulations of the joint dipole and quadruple waves to the simulations of the summary curve for the 2000 years, similar to that presented by Fig.6 in Zharkova et al. (2015). In Fig. 3 the summary curve with a quadruple wave with the amplitude a factor 0.3 of the dipole wave amplitude is presented in the top plot and the original summary curve derived for dipole waves from observations (Zharkova et al., 2015) in the bottom plot. It can be seen that the inclusion of a quadruple wave with smaller than the dipole wave amplitude affects the overall appearance of solar activity and allows us to detect some additional minima showing the occurrence of numerous seculiar minima in the past 800 years accounting for Gleissberg cycle (see Fig. 3, top plot).

### 4.2. Estimation of the quadruple source locations

Knowing the periods required for the quadruple waves to reproduce the observational periods and amplitudes of the seculiar (Gleissberg) minima, one can estimate the meridional flow magnitudes that can lead to the existence of waves with such the periods. The helioseismological data (Zhao et al., 2013) shows that the meridional flow is more intense closer to the surface. Hence, if the dynamo wave is generated with more intense meridional flow, then it has to be generated closer to the surface and vice versa. Also other helioseismic measurements of the physical conditions in deeper layers of the solar convection zone show the conditions favourable for exciting a quadrupole mode of poloidal magnetic field (Kryvodubskyj, 2001). Let us estimate our simulation results from this point of view.

In case of the absence of meridional circulation, or $v = 0$, for magnetic field with dipolar symmetry the harmonic oscillations are reproduced at $-220 < D < -100$, and for the magnetic field with the quadrupolar symmetry at $-410 < D < -110$. The period of magnetic field oscillations is smaller than the one observed in Sun. In order for our model to achieve the observed period of 22 years for solar activity, the model needs to include meridional flows with the magnitudes equal to several model units. Although, the dynamo numbers reproducing the dynamo waves with the period close to the required one for observed solar activity is not much different from the case with the absence of meridional flows.

On this reason, one can assume that the dynamo-numbers in all layers are the same and equal to $-170$ and calculate dipolar and quadrupolar magnetic field oscillations. Our calculations show that the period of these oscillations $T_1 = 21.41$ is achieved with $v \approx -2.6$ model units, $T_2 = 22.62$ with $v \approx -2.7$, and $T_3 = 27.24$ with $v \approx -2.56$. Hence, we discovered from the dynamo model that the meridional circulation in the layer generating the quadruple wave is directed against the direction of the wave motion. However, from the helioseimic observations of two cells (Zhao et al., 2013) shown in Fig. 4 of Zharkova et al. (2015) one can see that this situation with the opposite directions of meridional circulation and the direction of a quadrupole wave occurs only in the inner (deeper) layer allowing us to conclude that the quadruple wave origins from the inner layer located in the bottom of the SCZ.

## 5. Conclusions

In this paper we revised the previous prediction of solar activity for the past 800 years using a solar background magnetic field as the proxy of solar activity by the inclusion of magnetic waves produced by quadruple magnetic sources, in addition to the waves from the two-layer dipole sources previously reported (Zharkova et al., 2015).

For this purpose we apply the two layer dynamo model to produce the quadruple wave in the inner layer at the bottom of the SCZ with a period close but not eual to a normal 22 year solar cycle. The interference of this quadruple wave and two dipole waves with the periods of about 22 years leading to a grand cycle of about 400 years produce the double beating effect, which, in turn, leads to the additional minima of magnetic field occurring about every 100 years, called Gleissberg cycle.

Using the periods of the quadruple wave derived from the beating effect, we apply the dynamo model with the relevant meridional circulation to estimate the magnetic wave generated in the inner layer at the bottom of SCZ. This allows us to conclude that the SCZ is the most likely location where this qudruple wave has to be generated, in order to match to the observed timing and amplitude of the additional minima of Gleissberg's cycle in the grand cycles defined by a superposition of the dynamo waves generated in the inner and outer layers.

## Acknowledgement

The authors acknowledge with thanks that this work was initiated during the visit by EP to Northumbria University funded by the Royal Society grant RPJ02112, Investigation of solar activity with double dynamo waves: observations vs theory. This research was also partially funded by the grant ref. 16-17-10097 of Russian Science Foundation (PI-H. Popova).

## References

Babcock, H.W., Mar. 1961. The topology of the Sun's magnetic field and the 22-year cycle. Astrophys. J. 133, 572.
Bravo, S., González-Esparza, J.A., Mar. 2000. The north-south asymmetry of the solar and heliospheric magnetic field during activity minima. Geophys. Res. Lett. 27, 847–849.
Choudhuri, A.R., Chatterjee, P., Jiang, J., Mar. 2007. Predicting solar cycle 24 with a solar dynamo model. Phys. Rev. Lett. 98 (13), 131103.
Choudhuri, A.R., Chatterjee, P., Nandy, D., Nov. 2004. Helicity of solar active regions from a dynamo model. Astrophys. J. Lett. 615, L57–L60.
Choudhuri, A.R., Schussler, M., Dikpati, M., Nov. 1995. The solar dynamo with meridional circulation. Astron. Astrophys. 303, L29.
Dikpati, M., de Toma, G., Gilman, P.A., Mar. 2006. Predicting the strength of solar cycle 24 using a flux-transport dynamo-based tool. Geophys. Res. Lett. 33, 5102.
Dikpati, M., de Toma, G., Gilman, P.A., Arge, C.N., White, O.R., Feb. 2004. Diagnostics of polar field reversal in solar cycle 23 using a flux transport dynamo model. Astrophys. J. 601, 1136–1151.
Durney, B.R., Sep. 1995. On a Babcock-Leighton dynamo model with a deep-seated generating layer for the toroidal magnetic field. Sol. Phys. 160, 213–235.
Hathaway, D.H., Wilson, R.M., Reichmann, E.J., Dec. 2002. Group sunspot numbers: sunspot cycle characteristics. Sol. Phys. 211, 357–370.
Jennings, R.L., 1991. Symmetry breaking in a nonlinear -dynamo. Geophys. Astrophys. Fluid Dyn. 57, 147–189.
Jennings, R.L., Weiss, N.O., Sep. 1991. Symmetry breaking in stellar dynamos. Mon. Notices RAS 252, 249–260.
Karak, B.B., Nandy, D., Dec. 2012. Turbulent pumping of magnetic flux reduces solar cycle memory and thus impacts predictability of the Sun's activity. Astrophys. J. Lett. 761, L13.
Kryvodubskyj, V.N., 2001. Quadrupole mode of the Sun's poloidal magnetic field: on the possibility of exciting by turbulent dynamo mechanism. In: Brekke, P., Fleck, B., Gurman, J.B. (Eds.), Recent Insights into the Physics of the Sun and Heliosphere: Highlights from SOHO and Other Space Missions. Vol. 203 of IAU Symposium, p. 118.
Leighton, R.B., Apr. 1969. A magneto-kinematic model of the solar cycle. Astrophys. J. 156, 1.
Maris, G., Oncica, A., Mar. 2006. Solar cycle 24 forecasts. Sun Geosph. 1 (1), 010000–010011.
Muñoz-Jaramillo, A., Dasi-Espuig, M., Balmaceda, L.A., DeLuca, E.E., Apr. 2013. Solar cycle propagation, memory, and prediction: insights from a century of magnetic proxies. Astrophys. J. Lett. 767, L25.
Murayama, T., Nosaka, T., May 1991. Long-term variation in the north-south asymmetry of geomagnetic activity with respect to the solar equatorial plane. Planet. Space Sci. 39, 751–760.
Parker, E.N., Sep. 1955. Hydromagnetic dynamo models. Astrophys. J. 122, 293.
Parker, E.N., May 1993. A solar dynamo surface wave at the interface between convection and nonuniform rotation. Astrophys. J. 408, 707–719.
Pesnell, W.D., Oct. 2008. Predictions of solar cycle 24. Sol. Phys. 252, 209–220.

Popova, E., Zharkova, V., Zharkov, S., Nov. 2013. Probing latitudinal variations of the solar magnetic field in cycles 21-23 by Parker's Two-Layer Dynamo Model with meridional circulation. Ann. Geophys. 31, 2023–2038.

Popova, E.P., Apr. 2013. A dynamical system for the parker dynamo in the case of quadrupole symmetry of the magnetic field. Astron. Rep. 57, 310–315.

Ribes, J.C., Nesme-Ribes, E., Sep. 1993. The solar sunspot cycle in the Maunder minimum AD1645 to AD1715. Astron. Astrophys. 276, 549.

Schmidt, M., Lipson, H., Apr. 2009. Distilling free-form natural laws from experimental data. Science 324 (5923), 81–85.

Shepherd, S.J., Zharkov, S.I., Zharkova, V.V., Nov. 2014. Prediction of solar activity from solar background magnetic field variations in cycles 21-23. Astrophys. J. 795, 46.

Sokoloff, D., Nesme-Ribes, E., Aug. 1994. The Maunder minimum: a mixed-parity dynamo mode? Astron. Astrophys. 288, 293–298.

Solanki, S.K., Krivova, N.A., Nov. 2011. Analyzing solar cycles. Science 334, 916.

Solanki, S.K., Usoskin, I.G., Kromer, B., Schüssler, M., Beer, J., Oct. 2004. Unusual activity of the Sun during recent decades compared to the previous 11,000 years. Nature 431, 1084–1087.

Usoskin, I., Kovaltsov, G., 2015. A two-wave dynamo model by Zharkova et al. (2015) disagrees with data on long-term solar variability eprint arXiv:1512.05516.

Usoskin, I.G., Mursula, K., Solanki, S., Schüssler, M., Alanko, K., Jan. 2004. Reconstruction of solar activity for the last millennium using $^{10}$Be data. Astron. Astrophys. 413, 745–751.

Wang, Y.-M., Sheeley Jr., N.R., Nash, A.G., Dec. 1991. A new solar cycle model including meridional circulation. Astrophys. J. 383, 431–442.

Zhao, J., Bogart, R.S., Kosovichev, A.G., Duvall Jr., T.L., Hartlep, T., Sep. 2013. Detection of equatorward meridional flow and evidence of double-cell meridional circulation inside the Sun. Astrophys. J. Lett. 774, L29.

Zharkov, S., Gavryuseva, E., Zharkova, V., Apr. 2008. The observed long- and short-term phase relation between the toroidal and poloidal magnetic fields in cycle 23. Sol. Phys. 248, 339–358.

Zharkov, S.I., Zharkova, V.V., Feb. 2011. Statistical properties of H$\alpha$ flares in relation to sunspots and active regions in the cycle 23. J. Atmos. Sol. Terr. Phys. 73, 264–270.

Zharkova, V.V., Shepherd, S.J., Popova, E., Zharkov, S.I., Oct. 2015. Heartbeat of the Sun from Principal Component Analysis and prediction of solar activity on a millenium timescale. Nat. Sci. Rep. 5, 15689.

Zharkova, V.V., Shepherd, S.J., Popova, E., Zharkov, S.I., 2017. Reinforcing the double dynamo model with solar-terrestrial activity in the past three millennia eprint arXiv: 1705.04482.

Zharkova, V.V., Shepherd, S.J., Zharkov, S.I., Aug. 2012. Principal component analysis of background and sunspot magnetic field variations during solar cycles 21-23. Mon. Notices RAS 424, 2943–2953.